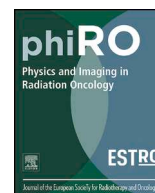




ELSEVIER

Contents lists available at ScienceDirect

# Physics and Imaging in Radiation Oncology

journal homepage: [www.elsevier.com/locate/phro](http://www.elsevier.com/locate/phro)

Original Research Article

## Comparison of tumor delineation using dual energy computed tomography versus magnetic resonance imaging in head and neck cancer re-irradiation cases



Sweet Ping Ng<sup>a,b,\*</sup>, Carlos E Cardenas<sup>c</sup>, Hesham Elhalawani<sup>a</sup>, Courtney Pollard III<sup>a</sup>, Baher Elgohari<sup>a</sup>, Penny Fang<sup>a</sup>, Mohamed Meheissen<sup>d</sup>, Nandita Guha-Thakurta<sup>e</sup>, Houda Bahig<sup>f</sup>, Jason M. Johnson<sup>e</sup>, Mona Kamal<sup>a</sup>, Adam S Garden<sup>a</sup>, Jay P. Reddy<sup>a</sup>, Shirley Y. Su<sup>g</sup>, Renata Ferrarotto<sup>h</sup>, Steven J. Frank<sup>a</sup>, G. Brandon Gunn<sup>a</sup>, Amy C. Moreno<sup>a</sup>, David I. Rosenthal<sup>a</sup>, Clifton D. Fuller<sup>a</sup>, Jack Phan<sup>a,\*</sup>

<sup>a</sup> Department of Radiation Oncology, The University of Texas MD Anderson Cancer Center, Houston, TX, USA

<sup>b</sup> Department of Radiation Oncology, Peter MacCallum Cancer Centre, Melbourne, Australia

<sup>c</sup> Department of Radiation Physics, The University of Texas MD Anderson Cancer Center, Houston, TX, USA

<sup>d</sup> Department of Clinical Oncology and Nuclear Medicine, University of Alexandria, Alexandria, Egypt

<sup>e</sup> Department of Diagnostic Imaging, The University of Texas MD Anderson Cancer Center, Houston, TX, USA

<sup>f</sup> Department of Radiation Oncology, Centre Hospitalier de l'Université de Montréal, Montreal, Quebec, Canada

<sup>g</sup> Department of Head and Neck Surgery, The University of Texas MD Anderson Cancer Center, Houston, TX, USA

<sup>h</sup> Department of Thoracic Head and Neck Medical Oncology, The University of Texas MD Anderson Cancer Center, Houston, TX, USA

### ARTICLE INFO

#### Keywords:

Re-irradiation  
Head and neck  
Dual energy computed tomography  
Magnetic resonance imaging  
Delineation

### ABSTRACT

In treatment planning, multiple imaging modalities can be employed to improve the accuracy of tumor delineation but this can be costly. This study aimed to compare the interobserver consistency of using dual energy computed tomography (DECT) versus magnetic resonance imaging (MRI) for delineating tumors in the head and neck cancer (HNC) re-irradiation scenario. Twenty-three patients with recurrent HNC and had planning DECT and MRI were identified. Contoured tumor volumes by seven radiation oncologists were compared. Overall, T1c MRI performed the best with median DSC of 0.58 (0–0.91) for T1c. T1c MRI provided higher interobserver agreement for skull base sites and 60 kV DECT provided higher interobserver agreement for non-skull base sites.

### 1. Introduction

Patients with recurrent head and neck cancer and a previous history of radiotherapy often pose a management dilemma. Local control is of importance in this group of patients, particularly in those with limited burden of distant disease, as progressive local disease can cause significant morbidity. Although local control can be achieved surgically, approximately 80% of patients with recurrent head and neck cancer are not surgical candidates [1]. Re-irradiation may be an option for these patients [2]. While previous studies have shown poor clinical outcomes and high toxicities in patients who received re-irradiation to the head and neck region [3–6], recent advancements in treatment planning and delivery (proton therapy, intensity modulated radiotherapy, stereotactic body radiotherapy) have prompted a renewed opportunity of

treating patients with re-irradiation [2]. The aim is to deliver high dose to the tumor to achieve good local control whilst limiting dose to surrounding normal tissue thereby reducing treatment-related toxicity.

In radiation treatment planning, multiple modality imaging can be employed to improve the accuracy of gross tumor volume (GTV) target delineation [7–10]. Accurate target delineation is particularly important in the re-irradiation scenario to avoid under-treatment of tumor or overtreatment of surrounding normal tissues. However, use of multiple imaging modalities can be costly. With an emphasis on a value-based approach, in this study we aimed to quantify the interobserver consistency of two imaging modalities, dual energy computed tomography (DECT) and magnetic resonance imaging (MRI) for delineating head and neck tumors for re-irradiation.

\* Corresponding authors at: The University of Texas MD Anderson Cancer Center, 1515 Holcombe Blvd, Houston, TX 77030, United States (J. Phan). Peter MacCallum Cancer Centre, 305 Grattan Street, Melbourne, Victoria, Australia (S.P. Ng).

E-mail addresses: [sweet.ng@petermac.org](mailto:sweet.ng@petermac.org) (S.P. Ng), [jphan@mdanderson.org](mailto:jphan@mdanderson.org) (J. Phan).

<https://doi.org/10.1016/j.phro.2020.04.001>

Received 12 March 2020; Received in revised form 16 April 2020; Accepted 21 April 2020

2405-6316/ © 2020 Published by Elsevier B.V. on behalf of European Society of Radiotherapy & Oncology. This is an open access article under the CC BY-NC-ND license (<http://creativecommons.org/licenses/by-nc-nd/4.0/>).

## 2. Materials and methods

### 2.1. Case selection

Patients with recurrent head and neck cancer treated definitively with re-irradiation at our institution and who underwent treatment planning with DECT (Discovery CT750 HD, GE Healthcare, Milwaukee, WI), and magnetic resonance imaging (MRI) (MR750 3 T MR system GE Healthcare, Milwaukee, WI) were retrospectively identified. MR studies included multiplanar T1, T2 with fat saturation, and T1 post contrast with fat saturation. The DECT and MRI scans were collected and used for this study under an Institutional Review Board approved protocol. The Institutional Review Board waived informed consent. DECT and MRI scans were performed in the radiation treatment position following CT simulation. Our DECT and MRI scanners were adapted to allow for the patients to be immobilized on the respective imaging device's couch using the patient-specific designed radiotherapy thermoplastic mask.

Twenty-three cases met the criteria for the study. Patient, tumour and treatment characteristics are summarized in Table 1 in [Supplementary material](#). All patients were treated using stereotactic body radiotherapy (SBRT) to the site of locoregional recurrence. Twelve of the cases involved skull base pathology and 11 cases were recurrent disease in mucosal or neck nodal sites (non-skull base).

Seven radiation oncologists contoured the GTV on the 60 kV and 140 kV images from the DECTs, and the T1 with contrast (T1c) and T2 images from the MRIs. The relevant clinical and tumor characteristics were provided to all observers. Observers contoured on each set of images at least a week apart to reduce recall bias.

### 2.2. Comparison of contours

Contours from each observer were extracted and compared for interobserver agreement using several metrics assessing overlap (Dice similarity coefficient, DSC), spatial distance (mean surface distance, MSD; 95th percentile Hausdorff distance, 95HD) and volume difference (VD). The definitions and formulae of these metrics are defined in [Supplementary material](#).

### 2.3. Statistical analysis

Pairwise comparisons between observers were used for each metric. The non-parametric Steel-Dwass test was used to compare all measurement pairs. Statistical analyses were performed using JMP software (version 14.0, 2018, SAS Institute Inc, Cary, NC).  $p$ -value of  $< 0.05$  was considered statistically significant.

## 3. Results

### 3.1. Overall pairwise analysis

The median recurrent tumor volume was 6.4 (range: 1–26)  $\text{cm}^3$ . As a group, there were no significant difference in volume difference of contoured tumor between the imaging modality and sequences. The overall median (range) of DSC for all imaging were 0.56 (0–0.88) for 60 kV, 0.53 (0–0.98) for 140 kV, 0.58 (0–0.91) for T1c and 0.45 (0–0.90) for T2. Steel-Dwass non-parametric comparison showed a significant difference in DSC between T1c and T2 ( $p < 0.0001$ ), T2 and 60kV ( $p < 0.0001$ ), 140kV and 60kV ( $p = 0.009$ ) and T1c and 140kV ( $p = 0.0015$ ). There was no significant difference between T1c and 60 kV ( $p = 0.898$ ), and T2 and 140 kV ( $p = 0.21$ ). As shown in [Fig. 1](#), there was less variability in DSC between observers in T1c and 60 kV.

On analysis of the spatial distance metrics, as depicted in [Fig. 1](#), there was less interobserver variability for T1c and 60 kV images. There was no significant difference between T1c and 60kV. When compared to other image sequences, there was significant difference between T1c

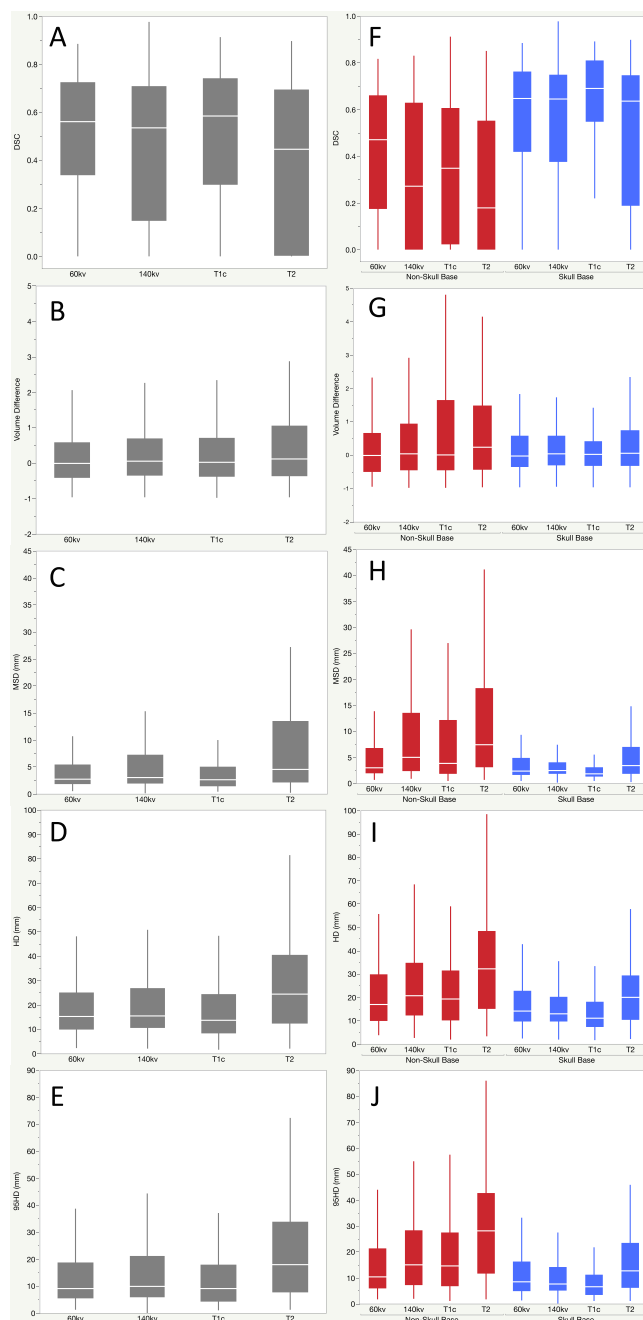


**Fig. 1.** Pairwise analysis for the cohort (A–E) and stratified by skull base versus non-skull base tumor sites (F–J): A and F) Dice similarity coefficient (DSC), B and G) volume difference, C and H) mean surface distance (MSD), D and I) Hausdorff distance (HD) and E and J) 95th percentile Hausdorff distance (95HD).

and 60 kV with 140 kV and T2 images. Similarly, T2 had higher HD and 95HD than other imaging sequences ( $p < 0.0001$  for all) ([Fig. 1](#)).

### 3.2. Skull base versus non-skull base target delineations

When analyzed separately, there was no VD difference noted in the skull base group. In the non-skull base group, there was significant VD between T2 MRI and 60 kV contours, with significantly larger VD in T2 than those in 60 kV images, with a median VD of 0.23 versus  $-0.01$  between observers ( $p = 0.03$ ) ([Fig. 2](#)).

The median DSC was higher in the skull base cases (0.65, range: 0–0.98) than the non-skull base cases (0.36, range: 0–0.91) ([Fig. 2](#)). In

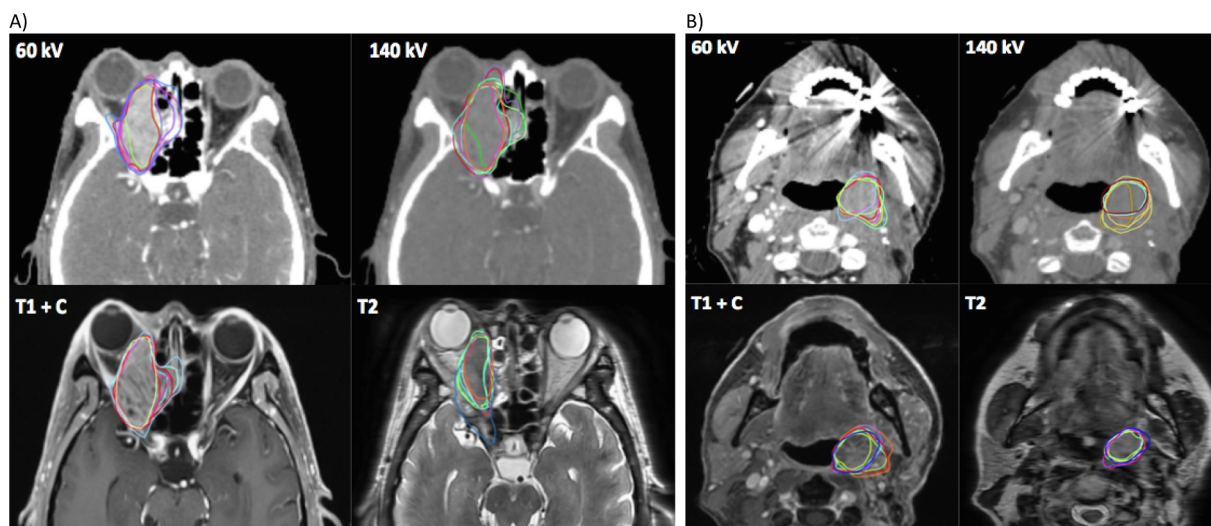


Fig. 2. Example of a skull base (A) and a non-skull base (B) cases with delineations on 60 kV, 140 kV, T1 with contrast (T1 + c) and T2 MRI sequences.

non-skull base cases, DSC was significantly higher in 60 kV (median: 0.47) as compared to 140 kV ( $p = 0.0013$ ), T1c ( $p = 0.032$ ) and T2 ( $p < 0.0001$ ). When comparing MR sequences, T1c had better DSC than T2 ( $p = 0.035$ ) in non-skull base cases. In skull base cases, T1c had significantly higher DSC than 60kV ( $p = 0.004$ ), 140kV ( $p < 0.001$ ) and T2 ( $p < 0.001$ ).

Overall, on spatial distance metrics, there was less variability in contours for all imaging sequences for skull base cases compared to non-skull base cases (Fig. 2). For skull base cases, the median MSD, HD and 95HD was lowest in T1c images and highest in T2. When T1c was compared to other sequences, there was significant difference in all. However, if comparing DECT sequences alone, there was no difference between 60 kV and 140 kV sequences for skull base cases. For non-skull base cases, there was no significant difference seen in MSD, 95HD and HD between T1c and DECT sequences (60 kV and 140 kV). T2 had higher variability between observers when compared to other sequences in both skull base and non-skull base cases.

#### 4. Discussion

Our results showed significant interobserver variability when measuring volumes' overlap and surface distance agreement, regardless of imaging modality in head and neck cancer cases which had previous radiotherapy. In some cases, there was complete disagreement (zero overlap) between two observer's tumor segmentations. This highlights the difficulty in assessing and delineating the target tumour in patients who had previous radiotherapy with/ without surgery due to soft tissue changes. For modern radiation treatment technique such as SBRT, in this cohort, which is highly precise with small planning target volume and a rapid dose falloff, small inaccuracies in target delineation can result in geographical misses.

Our analysis showed that on average T1c MRI sequence provided the most consistent delineations between observers, particularly in skull base cases. This is consistent with the current literature whereby skull base (extra/ intracranial) evaluations are preferred using T1c MR sequence. MRI is the imaging modality of choice for assessment of skull base due to the superior soft tissue contrast compared to CT imaging and is particularly useful for assessment of perineural disease [11–13]. Chung et al [8] demonstrated the usefulness of MRI in evaluating skull base disease in patients with nasopharyngeal carcinoma where MRI detected intracranial invasion in 96% of patients with pterygopalatine fossa involvement compared to 57% detection using CT imaging. The foramina and fissures of the skull base are often fat-filled and the differentiation between the fat pad and subtle disease can be challenging

due to the low attenuation differences between them. T1c MR imaging is often preferred for better visualization of disease in the skull base due to the hyperintensity of fat in this sequence compared to the tumor [13]. Although T2 MRI sequence was thought to be helpful in the characterization of tumor [11–13], our study has shown that there is high interobserver contour variability in the T2 sequences in the pre-irradiated cohort. Pre-existing changes from previous therapy coupled with tumor-related inflammation may have contributed to increased uncertainty and difficulty in interpreting the gross tumor border [14] thereby increasing interobserver variability in tumor delineation.

In non-skull base cases, 60 kV DECT may be adequate in aiding target delineation with the highest DSC between observers compared to other imaging sequences. This is consistent with other studies due to the considerable increase in iodine contrast attenuation at low energy providing improved lesion visibility compared to standard contrast-enhanced CT [15–18]. Although there is no consensus on optimal energy for soft tissue and tumor evaluation, the literature reported that energies of 40 kV to 60 kV have the highest tumor attenuation and are often the preferred energies for evaluation of head and neck malignancies [15–19]. These images can be obtained with no significant additional radiation dose to the patient compared to standard single-energy contrast-enhanced CT [20,21]. Literature assessing the utility of CT in head and neck predominantly concentrate on the delineation of non-skull base tumors [9,21,22] or normal soft tissue [21,23] and have found that the addition of MRI did not significantly alter the target delineation, consistent with our findings. Therefore, for non-skull base pathology, the use of low energy DECT images may be adequate in gross tumor delineation.

Our study showed that, in patients with previous irradiation of the head and neck region, T2-weighted sequences had the least interobserver agreement in target delineation. This may be secondary to the effect of previous radiation on the normal tissue, reducing the discrimination between pathology and normal tissue. The uncertainty of observers when contouring the tumor was also reflected in the resulted larger volumes of contours compared to 60 kV images in non-skull base cases. In a study comparing the volume of tumor delineated on MRI to histopathologic tumor volume by Jager et al. [24] found that the delineated tumor volumes on MRI were significantly larger than the true tumor volumes on histology. In our cohort of patients, previous irradiation resulting in fibrosis and scarring may obliterate normal soft tissue-fat planes making it challenging to discriminate between pathology and normal tissue [25,26]. Other factors may include previous surgical intervention and reconstruction (addition of tissue or surgical hardware) [26,27], tissue edema secondary to previous radiation

[14,25], and presence of tumor-related inflammation. Also, tumor recurrence can have similar radiological appearances on T2-weighted MR sequence as a vascularized scar [26].

Our study comes with its limitations. Firstly, this study was conducted in a high volume treatment center and the expertise and familiarity of observers with the interpretation of DECT and MRI may have reduced the magnitude of interobserver differences. In this study we chose to compare segmentations in a pairwise fashion to quantify variability extremes, which is not possible when using a STAPLE approach, which utilizes a computational algorithm to generate the ‘ground truth’ segmentation based on the collection of observers’ segmentations [28]. It could be argued that interobserver comparison to a generated STAPLE volume has the potential to significantly undermine the true variability between multiple observers. Secondly, although observers were only allowed to contour on each sequence set at least a week apart to reduce recall bias, there may be a mild degree of recall bias in some distinct cases, improving agreement between image sequences in those cases. By analyzing more than 10 cases in each skull base and non-skull base groups, we hoped the effect of recall bias was reduced. Thirdly, PET imaging was not evaluated in this study. In the setting of recurrent disease, PET imaging can help distinguish metabolically active tumor versus soft tissue or fibrosis. Multiple patients in this study did not have PET images available for assessment, and thus, PET could not be analyzed as part of this study.

Based on this study we recommend tumor and target volume segmentation peer-review since integrating this step into the clinical workflow could significantly impact the reduction of potential tumor misses [29]. It remains undetermined the role artificial intelligence will play in reducing target volume segmentation uncertainties; however, several works [30–33] have reported results which are encouraging and auto-segmentations could be used as guidance for radiation oncologists potentially reducing major misses. In summary, in this study, 60 kV DECT provided a higher interobserver agreement for non-skull base tumors, whereas T1c MRI provided a higher interobserver agreement for skull base tumors. For skull base tumors, the addition of T1c MRI may improve the accuracy of target delineation when available or not contraindicated. DECT can be utilized to aid target delineation of non-skull base tumors.

## Funding

This research did not receive any specific grant from funding agencies in the public, commercial, or not-for-profit sectors.

## Declaration of Competing Interest

The authors declare that they have no known competing financial interests or personal relationships that could have appeared to influence the work reported in this paper.

## Acknowledgements

Dr. Ng is funded by the Australian Postgraduate Award, RSNA Fellow Grant, and RANZCR research grants. Dr. Fuller is a Sabin Family Foundation Fellow. Dr. Fuller receives funding and salary support from the National Institutes of Health (NIH), including: the National Institute for Dental and Craniofacial Research Establishing Outcome Measures Award (1R01DE025248/R56DE025248) and an Academic Industrial Partnership Grant (R01DE028290); a National Science Foundation (NSF), Division of Mathematical Sciences, Joint NIH/NSF Initiative on Quantitative Approaches to Biomedical Big Data (QuBBDD) Grant (NSF 1557679); a National Institute of Biomedical Imaging and Bioengineering (NIBIB) Research Education Programs for Residents and Clinical Fellows Grant (R25EB025787-01); the NIH Big Data to Knowledge (BD2K) Program of the National Cancer Institute (NCI)

Early Stage Development of Technologies in Biomedical Computing, Informatics, and Big Data Science Award (1R01CA214825); NCI Early Phase Clinical Trials in Imaging and Image-Guided Interventions Program (1R01CA218148); an NIH/NCI Cancer Center Support Grant (CCSG) Pilot Research Program Award from the UT MD Anderson CCSG Radiation Oncology and Cancer Imaging Program (P30CA016672) and an NIH/NCI Head and Neck Specialized Programs of Research Excellence (SPORE) Developmental Research Program Award (P50CA097007). Dr. Fuller has received direct industry grant support, honoraria, and travel funding from Elekta AB.

## Appendix A. Supplementary data

Supplementary data to this article can be found online at <https://doi.org/10.1016/j.phro.2020.04.001>.

## References

- [1] Mabanta SR, Mendenhall WM, Stringer SP, Cassisi NJ. Salvage treatment for neck recurrence after irradiation alone for head and neck squamous cell carcinoma with clinically positive neck nodes. *Head Neck* 1999;21:591–4.
- [2] Ng SP, Phan J. Stereotactic radiotherapy and proton therapy for locally recurrent head and neck cancer. *Austin Head Neck Oncol* 2017;1:1002.
- [3] De Crevoisier R, Bourhis J, Domezge C, Wibault P, Koscielny S, Lusinchi A, et al. Full-dose reirradiation for unresectable head and neck carcinoma: experience at the Gustave-Roussy Institute in a series of 169 patients. *J Clin Oncol* 1998;16:3556–62.
- [4] Langer CJ, Harris J, Horwitz EM, Nicolaou N, Kies M, Curran W, et al. Phase II study of low-dose paclitaxel and cisplatin in combination with split-course concomitant twice-daily reirradiation in recurrent squamous cell carcinoma of the head and neck: results of Radiation Therapy Oncology Group Protocol 9911. *J Clin Oncol* 2007;25:4800–5.
- [5] Spencer SA, Harris J, Wheeler RH, Machtay M, Schultz C, Spanos W, et al. Final report of RTOG 9610, a multi-institutional trial of reirradiation and chemotherapy for unresectable recurrent squamous cell carcinoma of the head and neck. *Head Neck* 2008;30:281–8.
- [6] Strojjan P, Corry J, Eisbruch A, Vermorken JB, Mendenhall WM, Lee AW, et al. Recurrent and second primary squamous cell carcinoma of the head and neck: when and how to reirradiate. *Head Neck* 2015;37:134–50.
- [7] Bird D, Scarsbrook AF, Sykes J, Ramasamy S, Subesinghe M, Carey B, et al. Multimodality imaging with CT, MR and FDG-PET for radiotherapy target volume delineation in oropharyngeal squamous cell carcinoma. *BMC Cancer* 2015;15:844.
- [8] Chung NN, Ting LL, Hsu WC, Lui LT, Wang PM. Impact of magnetic resonance imaging versus CT on nasopharyngeal carcinoma: primary tumor target delineation for radiotherapy. *Head Neck* 2004;26:241–6.
- [9] Daisne JF, Duprez T, Weynand B, Lonnet M, Hamoir M, Reyckers H, et al. Tumor volume in pharyngolaryngeal squamous cell carcinoma: comparison at CT, MR imaging, and FDG PET and validation with surgical specimen. *Radiology* 2004;233:93–100.
- [10] Adams S, Baum RP, Stuckensen T, Bitter K, Hor G. Prospective comparison of 18F-FDG PET with conventional imaging modalities (CT, MRI, US) in lymph node staging of head and neck cancer. *Eur J Nucl Med* 1998;25:1255–60.
- [11] Badger D, Aygun N. Imaging of Perineural Spread in Head and Neck Cancer. *Radiol Clin North Am* 2017;55:139–49.
- [12] Parmar H, Gujar S, Shah G, Mukherji SK. Imaging of the anterior skull base. *Neuroimaging Clin N Am* 2009;19:427–39.
- [13] Kelly HR, Curtin HD. Imaging of skull base lesions. *Handb Clin Neurol* 2016;135:637–57.
- [14] Bharatha A, Yu E, Symons SP, Bartlett ES. Pictorial essay: early- and late-term effects of radiotherapy in head and neck imaging. *Can Assoc Radiol J* 2012;63:119–28.
- [15] Forghani R, Mukherji SK. Advanced dual-energy CT applications for the evaluation of the soft tissues of the neck. *Clin Radiol* 2018;73:70–80.
- [16] Albrecht MH, Scholtz JE, Kraft J, Bauer RW, Kauf M, Dewes P, et al. Assessment of an Advanced Monoenergetic Reconstruction Technique in Dual-Energy Computed Tomography of Head and Neck Cancer. *Eur Radiol* 2015;25:2493–501.
- [17] Lam S, Gupta R, Levental M, Yu E, Curtin HD, Forghani R. Optimal Virtual Monochromatic Images for Evaluation of Normal Tissues and Head and Neck Cancer Using Dual-Energy CT. *AJNR Am J Neuroradiol* 2015;36:1518–24.
- [18] Tawfik AM, Kerl JM, Bauer RW, Nour-Eldin NE, Naguib NN, Vogl TJ, et al. Dual-energy CT of head and neck cancer: average weighting of low- and high-voltage acquisitions to improve lesion delineation and image quality-initial clinical experience. *Invest Radiol* 2012;47:306–11.
- [19] May MS, Wiesmueller M, Heiss R, Brand M, Bruegel J, Uder M, et al. Comparison of dual- and single-source dual-energy CT in head and neck imaging. *Eur Radiol* 2018.
- [20] Tawfik AM, Kerl JM, Razeq AA, Bauer RW, Nour-Eldin NE, Vogl TJ, et al. Image quality and radiation dose of dual-energy CT of the head and neck compared with a standard 120-kVp acquisition. *AJNR Am J Neuroradiol* 2011;32:1994–9.
- [21] Scholtz JE, Kauf M, Kraft J, Noske EM, Scheerer F, Schulz B, et al. Objective and subjective image quality of primary and recurrent squamous cell carcinoma of head and neck low-tube-voltage 80-kVp computed tomography. *Neuroradiology*

- 2015;57:645–51.
- [22] Thiagarajan A, Caria N, Schoder H, Iyer NG, Wolden S, Wong RJ, et al. Target volume delineation in oropharyngeal cancer: impact of PET, MRI, and physical examination. *Int J Radiat Oncol Biol Phys* 2012;83:220–7.
- [23] Geets X, Daisne JF, Arcangeli S, Coche E, De Poel M, Duprez T, et al. Inter-observer variability in the delineation of pharyngo-laryngeal tumor, parotid glands and cervical spinal cord: comparison between CT-scan and MRI. *Radiother Oncol* 2005;77:25–31.
- [24] Jager EA, Ligtenberg H, Caldas-Magalhaes J, Schakel T, Philippens ME, Pameijer FA, et al. Validated guidelines for tumor delineation on magnetic resonance imaging for laryngeal and hypopharyngeal cancer. *Acta Oncol* 2016;55:1305–12.
- [25] Hermans R. Post-treatment imaging of head and neck cancer. *Cancer Imaging*; 2004: 4 Spec No A:S6-S15.
- [26] Saito N, Nadgir RN, Nakahira M, Takahashi M, Uchino A, Kimura F, et al. Posttreatment CT and MR imaging in head and neck cancer: what the radiologist needs to know. *Radiographics*. 2012; 32: 1261-82; discussion 82-4.
- [27] Ng SP, Dyer BA, Kalpathy-Cramer J, Mohamed ASR, Awan MJ, Gunn GB, et al. A prospective in silico analysis of interdisciplinary and interobserver spatial variability in post-operative target delineation of high-risk oral cavity cancers: Does physician specialty matter? *Clin Transl Radiat Oncol* 2018;12:40–6.
- [28] Warfield SK, Zou KH, Wells WM. Simultaneous truth and performance level estimation (STAPLE): an algorithm for the validation of image segmentation. *IEEE Trans Med Imaging* 2004;23:903–21.
- [29] Cardenas CE, Mohamed ASR, Tao R, Wong AJR, Awan MJ, Kuruvila S, et al. Prospective Qualitative and Quantitative Analysis of Real-Time Peer Review Quality Assurance Rounds Incorporating Direct Physical Examination for Head and Neck Cancer Radiation Therapy. *Int J Radiat Oncol Biol Phys* 2017;98:532–40.
- [30] Cardenas CE, McCarroll RE, Court LE, Elgohari BA, Elhalawani H, Fuller CD, et al. Deep Learning Algorithm for Auto-Delineation of High-Risk Oropharyngeal Clinical Target Volumes With Built-In Dice Similarity Coefficient Parameter Optimization Function. *Int J Radiat Oncol Biol Phys* 2018;101:468–78.
- [31] Huang B, Chen Z, Wu PM, Ye Y, Feng ST, Wong CO, et al. Fully automated delineation of gross tumor volume for head and neck cancer on PET-CT using deep learning: a dual-center study. *Contrast Media Mol Imaging* 2018;2018:8923028.
- [32] Cardenas CE, Anderson BM, Aristophanous M, Yang J, Rhee DJ, McCarroll RE, et al. Auto-delineation of oropharyngeal clinical target volumes using 3D convolutional neural networks. *Phys Med Biol* 2018;63:215026.
- [33] Men K, Chen X, Zhang Y, Zhang T, Dai J, Yi J, et al. Deep Deconvolutional neural network for target segmentation of nasopharyngeal cancer in planning computed tomography images. *Front Oncol* 2017;7:315.



Minerva Access is the Institutional Repository of The University of Melbourne

**Author/s:**

Ng, SP; Cardenas, CE; Elhalawani, H; Pollard, C; Elgohari, B; Fang, P; Meheissen, M; Guha-Thakurta, N; Bahig, H; Johnson, JM; Kamal, M; Garden, AS; Reddy, JP; Su, SY; Ferrarotto, R; Frank, SJ; Brandon Gunn, G; Moreno, AC; Rosenthal, DI; Fuller, CD; Phan, J

**Title:**

Comparison of tumor delineation using dual energy computed tomography versus magnetic resonance imaging in head and neck cancer re-irradiation cases

**Date:**

2020-04-01

**Citation:**

Ng, S. P., Cardenas, C. E., Elhalawani, H., Pollard, C., Elgohari, B., Fang, P., Meheissen, M., Guha-Thakurta, N., Bahig, H., Johnson, J. M., Kamal, M., Garden, A. S., Reddy, J. P., Su, S. Y., Ferrarotto, R., Frank, S. J., Brandon Gunn, G., Moreno, A. C., Rosenthal, D. I. ,... Phan, J. (2020). Comparison of tumor delineation using dual energy computed tomography versus magnetic resonance imaging in head and neck cancer re-irradiation cases. *Physics and Imaging in Radiation Oncology*, 14, pp.1-5. <https://doi.org/10.1016/j.phro.2020.04.001>.

**Persistent Link:**

<http://hdl.handle.net/11343/252591>

**File Description:**

Published version

**License:**

cc-by-nc-nd